Published in final edited form as:
Comput Phys Commun. 2010 December 1; 181(12): 2001–2007. doi:10.1016/j.cpc.2010.08.029.

A model for Structure and Thermodynamics of ssDNA and dsDNA Near a Surface: a Coarse Grained Approach

J. Ambia-Garrido[1], **Arnold Vainrub**[2], and **B. Montgomery Pettitt**[1]

[1] Department of Physics and Department of Chemistry, University of Houston, Houston, Texas

[2] College of Veterinary Medicine, Auburn University, Auburn, AL 36849

Abstract

New methods based on surfaces or beads have allowed measurement of properties of single DNA molecules in very accurate ways. Theoretical coarse grained models have been developed to understand the behavior of single stranded and double stranded DNA. These models have been shown to be accurate and relatively simple for very short systems of 6–8 base pairs near surfaces. Comparatively less is known about the influence of a surface on the secondary structures of longer molecules important to many technologies. Surface fields due to either applied potentials and/or dielectric boundaries are not in current surface mounted coarse grained models. To gain insight into longer and surface mounted sequences we parameterized a discretized worm-like chain model. Each link is considered a sphere of 6 base pairs in length for dsDNA, and 1.5 bases for ssDNA (requiring an always even number of spheres). For this demonstration of the model, the chain is tethered to a surface by a fixed length, non-interacting 0.536 *nm* linker. Configurational sampling was achieved via Monte-Carlo simulation. Our model successfully reproduces end to end distance averages from experimental results, in agreement with polymer theory and all atom simulations. Our average tilt results are also in agreement with all atom simulations for the case of dense systems.

1 Introduction

In the last couple of decades, the importance of understanding the fundamental properties of DNA has been propelled by the human genome project and the now routine use of next generation sequencers [1]. Many new technologies involve short DNA strands tethered to different surfaces or particles. There has been an effort to understand the associated phenomena from a theoretical point of view [2,3,4,5,6,7,8,9,10,11,12,13]. Such efforts are of use in experimental design as well as analysis. In particular, the electrostatic surface fields due to either applied potentials or dielectric boundaries have been incorporated into a qualitative thermodynamic theory of hybridization on surfaces [3,4,14,15] which has been used to understand the optimal performance of DNA microarrays [16,17,18] as well as of DNA-nanoparticles assemblies [19,20].

While simulations have been used to consider geometric factors, analytic theory has been used to understand the shift in binding energy and melting temperature for DNA hybridizing near a surface. To date analytical evaluations of the electrostatic interaction have been limited to 8 base pair long DNA fragments. [3,4,14,15] There is a clear need to extend the

methods to systems which are longer and may include various single stranded, unpaired overhangs to better analyze surface mounted experiments.

Here we propose a new model for arbitrarily long oligonucleotides that includes the electrostatic interaction between the DNA strand(s) and the surface. The model does attempt to capture hybridization (or melting) dynamics[8] but seeks to accurately incorporate the effects on thermodynamics of target and probe strands of differing lengths, on surfaces either dielectric or metalic and to better model finite surface concentration effects. The coarse grained model we propose in this work also includes the bending rigidity of the molecule, which varies significantly between single stranded DNA and double stranded DNA. To capture the remaining conformational/entropic components of the free energy, we sample configurations of the coarse grained chain with a Metropolis Monte Carlo algorithm. Comparisons with polymer theory and explicit all atom simulations in selected cases provide the validation for the model [5,6]. Our methods are also compared and in agreement with experimental measurements available in the literature [21,22,23,24,25,26,27].

2 Model

We take a discretized version of the worm-like chain model with coarse grained dimensions as our basic framework. The DNA molecule in either single stranded (ssDNA) or double stranded (dsDNA) form is to be considered as a chain of spheres. If we are modeling dsDNA, the spheres have a 1 nm radius r_0, whereas the ssDNA case has a 0.5 *nm* radius. Since the average distance between bases is 0.34 *nm* for dsDNA and 0.63 *nm* for ssDNA, the dsDNA sphere models 6 base pairs and the single stranded sphere models 1.5 bases. To maintain a discrete number of base pairs, we always have an even number of spheres in the ssDNA case (modeling 3 base pairs for every 2 spheres). The chain flexibility depends on the persistence length of the molecule and was parameterized as a chain bending energy accordingly [21,28,29,23]. The molecules interact electrostatically in a dielectric continuum solvent with the surface and with other molecules when present.

Our effective energy model may be written as

$$E_{Total}=E_{Bending}+E_{Surface}+E_{Neighbors} \tag{1}$$

The energy required to bend a segment of length L through an angle θ is calculated using a simple elastic rod model [23,30]:

$$E_{Bending}=\frac{k_B TP}{2L}\theta^2=\frac{k_B TPL}{2R^2} \tag{2}$$

Where k_B is Boltzmann's constant, T is the temperature (25 °C), P is the persistence length and R is the radius of curvature. The persistence length depends on the salt concentration of the liquid in which the molecule is submerged and is different for ssDNA and for dsDNA. For dsDNA, Baumann et al. [22], proposed the following formula:

$$P=P_0^{ds}+\frac{1}{4\kappa^2 l_B}=P_0^{ds}+\frac{0.0324}{I} \tag{3}$$

Where $P_0^{ds}=50\ nm$ for dsDNA, $\frac{1}{\kappa}$ is the Debye-Hückel screening length, l_B is the Bjerrum length and I is the ionic strength, which equals the ion concentration for monovalent ions

like Na^+. The constant 0.0324 is in *nm*. In the case of ssDNA, we use the same mathematical model for the data given by Murphy et al [24] and Tinland et al [31]. Now P_0^{ss}=1.481 *nm*, and

$$P=P_0^{ss}+\frac{0.03797}{I} \tag{4}$$

In our model we consider the DNA molecules immersed in a saline solution. The effective electrostatic interactions are reasonably, approximately described by a Poisson-Boltzmann approach as is done with the Gouy-Chapman double layer theory [32,33]. The electric permittivity of water at 25°C is 78.54 ε_0 [34]. Each sphere will be considered ion permeable [35,36], with the charge distributed on the surface. This description was previously used by Vainrub and Pettitt [2,3] as justified by the results of simulation densities for ions within the grooves of dsDNA [37,38]. The total charge on each sphere depends on the molecule (ssDNA or dsDNA): Q_{ds} = 12 e^- and Q_{ss} = 1.5 e^-.

We consider two types of commonly used surfaces: dielectrics and conductors. Examples in routine use would include SiO_2 glass and gold respectively. These two types of materials have dramatically different surface effects. If the surface is a dielectric, it will keep a constant charge density. On the other hand, if the surface is a conductor, it will keep a constant electric potential (voltage). There are various ways to achieve these fields in the laboratory using both external sources and by modifying the surface with either acidic (negatively charged) or basic (positively charged) groups. To consider these cases, we use the common electrostatic method of images. If we are dealing with a dielectric, each sphere near the surface will have an image in the solid with the same charge. While if the surface is a conductor, the image sphere will have opposite charge. Given this boundary condition imposed by the surface, we may phrase this in terms of a fixed voltage V (conductor) or charge distribution σ (dielectric). The effective energy due to the surface is simply half the integral of the charge times the electric potential over the surface and over the sphere volumes.

$$E_S=\frac{1}{2}\int_{plane}\sigma\psi\, dS+\frac{1}{2}\int_{sphere}\rho\psi\, dV \tag{5}$$

For a delta charge distribution in the surface, we get for each sphere (next to a conductor or dielectric surface) [2,3]:

$$E_{cS}=-\frac{\alpha}{\varepsilon\varepsilon_0\kappa}\left[\frac{V\varepsilon\varepsilon_0\kappa}{2}e^{-\kappa z}+\sum_i\frac{\kappa\alpha}{8\pi l_i}e^{-\kappa l_i}\right] \tag{6}$$

$$E_{dS}=-\frac{\alpha}{\varepsilon\varepsilon_0\kappa}\left[\sigma e^{-\kappa z}-\sum_i\frac{\kappa\alpha}{8\pi l_i}e^{-\kappa l_i}\right] \tag{7}$$

where the constant

$$\alpha = \frac{Q \sinh(\kappa r_0)}{\kappa r_0}$$

Where z is the distance between the center of the sphere and the plane and l is the distance between the centers of the sphere and the image sphere; i runs over all image spheres. Finally, the energy due to possible neighbors is the same integral used for the image spheres, but the result doubles because both spheres are real.

$$E_N = \frac{\alpha^2}{8\pi\varepsilon\varepsilon_0}\left[\sum_j \frac{2e^{-\kappa l_j}}{l_j} - \sum_i \frac{e^{-\kappa l_i}}{l_i}\right] \quad (8)$$

Here j runs over all spheres in neighboring strands and i runs over all image spheres of the neighboring strands.

Chemically, the DNA molecule is tethered to the surface by a neutral epoxide chain, as is common use in experiments and molecular simulations [5,6]. The linker is modeled as a short chain of two neutral spheres with a persistence length of 0.76 *nm* [39]. Each sphere has a 0.134 *nm* radius for a total chain length of 0.536 *nm*. We note that the use of charged linkers is easily modeled with our method.

3 Monte Carlo Simulation

The flexible chains may take a variety of conformations whose distribution must be determined by simulation. In our simulation we used a Metropolis Monte Carlo algorithm to sample the configurations of the chains. The initial configuration is random, making sure we have no overlaps. Then we let the system evolve by the well known “kink jump” algorithm, proposed by Baumgärtner and Binder [40]. In this algorithm, a sphere is chosen at random and moved around the axis connecting the neighboring spheres by a random angle. If the sphere is at the end of the chain, we choose a solid angle and simply rotate it keeping the distance to the neighbor fixed. At this point we recalculate the energy of the system and choose to either keep the new configuration or reject it, using the standard Metropolis criterion. All spheres have an equal probability to be chosen, and we count as step when N spheres have attempted to move.

We ran the described simulation for a single molecule, and for arrays of molecules. Each simulation was run for 10,000,000 production steps. Using energetic considerations the MC equilibration time was never more than 10,000 steps.

4 Results

A number of structural measures are relevant for comparison with previous theory, all atom simulation and experiments. We computed the end to end distance and the tilting angle dependence on the salt concentration, the number of base pairs and the surface concentration. These are measures where quantitative comparisons can be made. Some insight was gained by considering the variation of the contributions among the different effective energy sources, to better understand the dominating interactions in the model.

4.1 Single Molecule

In Fig. 2 we see how the average end to end distance depends on the number of base pairs of the molecule for different conditions of the surface, and without surface. Since dsDNA is relatively rigid (>50 *nm* persistence length), we see an essentially monotonic increase, independent of the surface presence or condition.

For a small number of base pairs, the ssDNA has a longer end to end distance than dsDNA, which is expected because ssDNA has a 0.64 *nm* distance between base pairs, while dsDNA only has 0.34 *nm*. However, for more base pairs, ssDNA has a shorter end to end distance than dsDNA, because it curls over on itself much more on average, due to its shorter persistence length (≈ 1.48 *nm*). For the ssDNA, we can also see that the average end to end distance, and its fluctuations, are affected by the conditions of the near surface. The results show we have the shortest end to end distance when we have no surface in agreement with analytic theory, and the longest for a dielectric surface with a charge of $-0.36\ e^-$ per nm^2 (effectively a positive charge). If we decrease the salt concentration, the effect is stronger; while if we increase the salt concentration, the electrostatic screening is stronger and the molecules will ultimately behave like if the only surface interaction was excluded volume (case (A) in Fig. 2). The fluctuation is relatively small for dsDNA due to its high rigidity, but in the ssDNA case it is increased when we have a charge or a voltage on the surface. Having a larger fluctuation, in the structure of the tethered probe molecules, could be an advantage in a hybridization experiment, because it means more of the conformational space is covered, facilitating the hybridization. This includes both angle and end to end distance.

Now we briefly discuss the role of exclude volume interactions and the monomer-monomer and monomer-surface electrostatic interactions. Classical theoretical result for the mean end-to-end distance square average $\langle R^2 \rangle$ of the polymer chain with N segments [41,42] no encumbered by a surface show:

$$\langle R^2 \rangle \sim N^{2\nu} \tag{9}$$

where the exponent ν is given by

$$\nu = \frac{3}{d+2} \tag{10}$$

and where d is the dimensionality of the space.

When $d = 3$, for a free, linear macromolecule (not attached to any surface) dissolved in a good solvent, $2\nu = 1.2$; and when $d = 2$, $2\nu = 1.5$, which is the case for two dimensions, hence a strong confinement. Formally, in the intermediate case of chain molecule attachment by one-end to the surface $2 < d < 3$ and thus $1.2 < 2\nu < 1.5$. The Monte Carlo simulation results in Fig. 2 were fitted by Eq. 9 and the obtained effective exponents for the ssDNA case are shown in Table 1. We find all simulated data sets are fit accurately with an error below 1 – 2%. For a non tethered chain the fitting gives the full exponent $2\nu = 1.20$ in strict agreement with theory. For the attractive conductor surface $2\nu = 1.258$ is larger and grows further to 1.294 when the attraction is enhanced by the applied positive potential. The behavior tends to the $d = 2$ case as a result of weak electrostatic adsorption of the DNA molecules to the surface, namely an effective confinement. This effect is most drastic when the dielectric surface has a charge of $-0.36 e^-/nm^2$ and attracts the DNA molecule. This confines the motion to a conformation parallel to the surface and thus results in an increase

of the effective exponent v from $d = 3$ value $2v = 1.2$ towards $d = 2$ value 1.5. Therefore, the simulation data are in excellent scaling agreement with mean-field theory Eqs. 9 and 10.

In Fig. 3, we show a plot of tilt angle vs. salt concentration for ssDNA and dsDNA near different surfaces. A 0° angle means the strand is perpendicular to the surface and a 90° angle means parallel. Both ssDNA and dsDNA show changes depending on the surface conditions. We can see how all experiments for ssDNA tend to an average angle of roughly 57° when the salt concentration is high and the electrostatic interaction is weaker. This angle can be compared with the random orientation case, where the average tilt is

$$\langle\theta\rangle=\int_0^{\pi/2}\theta sin(\theta)d\theta=57.3^\circ \tag{11}$$

The large fluctuations shown in Fig. 3 are indicative of the configuration space coverage for this system.

For the dsDNA, we see a different behavior than for the single stranded. The tilt angle apparently converges for higher salt concentrations around ≈ 40° and the fluctuation is ≈ 5° smaller. This can be explained by the stronger electrostatic interaction, and the bigger size, hence more excluded volume.

For molecules with more base pairs, the electrostatic interaction will be stronger. In most cases studied here the interaction between the surface and the molecule is attractive and we expect an angle closer to 90°. Interestingly enough, this did not happen for the ssDNA case (up to 36 base pairs) near a conducting surface.

To analyze the importance of the interactions in the system, we separate the energy contributions in equation 1, and further separating $E_{Surface}$ into a contribution due to the conditions that the surface imposes by its nature, the polarization field or image charges from an analytical point of view, and a contribution due to the bare charge or the voltage in the surface.

$$E_{Total}=E_{Bending}+E_{Images}+E_{Charge/Voltage}+E_{Neighbors} \tag{12}$$

We plot some results in figures 4 and 5. As expected, in the dsDNA case, we have an electrostatic dominated system for medium and low salt concentrations. At high salt we have a transition to a elastically dominated system. The electrostatic contribution is only significant for very low salt concentrations due to screening.

We note that the fluctuations for the dsDNA near any surface with some attractive interaction (all but a simple dielectric) shows a maximum at ≈0.15M (e. g. Fig. 5). We have attributed this behavior to a competition for the dominant energy contribution. This behavior has not been reported to our knowledge for ssDNA near a surface. While it seems universal in our context, it may be specific due to our approximations. We hope to provoke our experimental collaborators to test this by scanning the intensity over a range of salt dilutions on a single attractive surface chip.

If we increase the number of base pairs, $E_{Bending}$ and $E_{Charge/V oltage}$ increase almost linearly until up to 36 base pairs. Nonetheless, E_{Images} shows little change.

4.2 Many Molecules: surface crowding

We now consider the problems of surface coverage in a microarray or microbead system. We consider a piece of the system and use periodic boundary conditions on the unit cell. In this case we model a 10×10 hexagonal unit lattice of probes, with periodic boundary conditions. We ran the simulation for 4 different molecular surface densities: 0.01, 0.10, 0.15 and 0.20 *molecules/nm*^{2}. Up to 4th neighbors were considered in the interaction energies.

When the molecular surface density is low (0.01 *molecules* per *nm*^{2}) and the distance between probe molecules is bigger than the end to end distance of the molecules, the results are evidently very similar to the case when we have only one DNA molecule. However, a different behavior is observed as the surface density or the number of base pairs grows. As expected, the end to end distance for dsDNA is not affected because of its stiffness, while ssDNA shows an increase of its end to end distance, proportional to the closeness of the neighbors, which is never shorter than its dsDNA counterpart (for the same number of base pairs), see Fig. 6.

For the tilt angle, in all surface conditions, we see a significant shift as the surface molecular density increases. Not surprisingly, the closer they get, the more perpendicular to the surface they tend to remain. This is because they repel each other through charge and excluded volume. However, they do not seem to converge to a 0° angle. As an example we show the case of a surface with a 50 *mV* voltage in Fig. 7. Similar phenomena were previously observed by all atom simulations performed by Wong and Pettitt [5,6], by Schatz and Lee [9] and by Jiang et. al. [10].

Experimentally, the average tilt angle was studied for DNA tethered to gold [25,43], silicon dioxide [26] and diamond [27] surfaces. The results for the conducting surface in Fig. 7 are in qualitative agreement with the tilt measurements of DNA attached to gold. For example, the tilt angle is 45° for 15 base pair long dsDNA in 0.1 M potassium phosphate solution [25], but a quantitative comparison with the theory in Fig. 7 is hindered due to an uncertain probe surface density in the experiment.

The DNA tilt distribution can be better understood when we consider the 2nd moment or fluctuation as it also increases (for low salt) when the molecules get closer (higher density). While the molecules fluctuate much more, they have an average position with a higher tilt angle. The linker also helps them effectively stay further from each other.

In analyzing the energy contributions we find E_{Image} increases very slightly, but not enough to be considered a significant effect. $E_{Bending}$, decreases a little because the neighbors restrain the molecule to a smaller space. For low surface densities, $E_{Neighbors}$ is too small to be considered a major effect. As we increase the density, $E_{Neighbors}$ gains importance, especially for the dsDNA case, where it can be the dominant energy contribution as shown in Fig. 8 and Fig. 9.

The fluctuations behave almost the same way the average energy does, for the ssDNA case. But for the dsDNA case, we see a different trend. We find a maximum in the total energy's fluctuation, located at about the same surface density where the system transitions from being elastically dominated to electrostatically dominated.

5 Conclusions

Many effects, both equilibrium and kinetic, are important to consider in modeling nucleic acids near surfaces. All atom simulations for the number of systems we presented here

would be unreasonably computationally expensive. Here we demonstrated a simple, coarse grained model that can successfully reproduce experimental, and all-atom simulation results requiring very modest computational power. The model proved capable of providing nontrivial insights in surface mounted cases where the target and probe lengths differ and gave us access to a wide variety of conditions with minimal computational effort. This simulation model should be useful in the improvement of surface mounted technologies.

There are a number of system variables that can be adjusted in this computational model relevant to chip design. This model and the results can be used to analyze the hybridization efficiency as well as the melting temperature curve for hybridizing systems near a surface for a variety of systems. The model in its current form should be capable of helping with the analysis of experimental microarray data and we will test this in the near future.

Acknowledgments

JAG was partially supported by a training fellowship from the Keck Center for Interdisciplinary Bioscience Training of the Gulf Coast Consortia. The Robert A. Welch Foundation (E-1028), and the National Institutes of Health (GM-066813) are thanked for partial support of this work. This research was performed in part using the Molecular Science Computing Facility in the William R. Wiley Environmental Molecular Sciences Laboratory, located at the Pacific Northwest National Laboratory and in part by the National Science Foundation through TeraGrid resources provided by Pittsburgh Supercomputing Center.

References

1. Benham C, Mielke S. Dna mechanics. Annu Rev Biomed Eng 2005;7:21–53. [PubMed: 16004565]
2. Vainrub A, Pettitt BM. Thermodynamics of association to a molecule immobilized in an electric double layer. Chem Phys Lett 2000;323:160–166.
3. Vainrub A, Pettitt BM. Coulomb blockage of hybridization in two-dimensional dna arrays. Phys Rev E 2002;66:041905.
4. Vainrub A, Pettitt BM. Sensitive quantitative nucleic acid detection using oligonucleotide microarrays. J Am Chem Soc 2003;125:7798–7799. [PubMed: 12822987]
5. Wong K, Pettitt BM. A study of dna tethered to a surface by an all-atom molecular dynamics simulation. Theor Chem Acc 2001;106:233–235.
6. Wong K, Pettitt BM. Orientation of dna on a surface from simulation. Biopolymers 2004;73:570–578. [PubMed: 15048781]
7. Lynch G, Qamhieh K, Wong K, Pettitt BM. The melting mechanism of dna tethered to a surface. IJNAM 2009;6:474–488.
8. Hall C, Jayaraman A, Genzer. Computer simulation study of probe-target hybridization in model dna microarrays: Effect of probe surface density and target concentration. J Chem Phys 2007;127:144912. [PubMed: 17935444]
9. Lee O, Schatz GC. Interaction between dnas on a gold surface. J Phys Chem C 2009;113:15941–15947.
10. Hower J, He Y, Yao L, Sullivan J, Jiang S. Packing structures of single-stranded dna and double-stranded dna thiolates on au(111): A molecular simulation study. J Chem Phys 2007;127:195101. [PubMed: 18035905]
11. Gong P, Levicky R. Dna surface hybridization regimes. Proc Natl Acad Sci USA 2008;105(14):5301–5306. [PubMed: 18381819]
12. Chattopadhyay AK, Marenduzzo D. Dynamics of an anchored polymer molecule under an oscillating force. PRL 2007;98:088101.
13. Buhot A, Halperin A, Zhulina EB. Sensitivity, specificity, and the hybridization isotherms of dna chips. Biophysical Journal 2004;86:718–730. [PubMed: 14747310]
14. Vainrub A, Pettitt BM. Surface electrostatic effects in oligonucleotide microarrays: Control and optimization of binding thermodynamics. Biopolymers 2003;68:265–270. [PubMed: 12548628]

15. Vainrub A, Pettitt BM. Theoretical aspects of genomic variation screening using dna microarrays. Biopolimers 2004;73:614–620.
16. Dufva M. Fabrication of high quality microarrays. Biomolecular Engineering 2005;22:173–184. [PubMed: 16242381]
17. Langdon WB, Upton GJG, Harrison AP. G-spots cause incorrect expression measurement in affymetrix microarrays. BMC Genomics 2008;9:613. [PubMed: 19094220]
18. Steinberg KM, Hagen K, Athri P, Shetty AC, Patel V, Okou DT, Locke AE, Zwick ME. Combining microarray-based genomic selection (mgs) with the illumina genome analyzer platform to sequence diplod target regions. Annals of Human Genetics 2009;73:502–513. [PubMed: 19573206]
19. Xu J, Craig SL. Thermodynamics of dna hybridization on gold nanoparticles. JACS 2005;127:13227–13231.
20. Harris NC, Kiang C. Defects can increase the melting temperature of dna-nanoparticle assemblies. J Phys Chem B 2006;110:16393–16396. [PubMed: 16913768]
21. Finzi L, Smith SB, Bustamante C. Direct mechanical measurements of the elasticity of single dna molecules by using magnetic beads. Science 1992;258:1122–1126. [PubMed: 1439819]
22. Bloomfield V, Baumann CG, Smith SB, Bustamante C. Ionic effects on the elasticity of single dna molecules. Proc Natl Acad Sci USA 1997;94:6185–6190. [PubMed: 9177192]
23. Bryant Z, Bustamante C, Smith SB. Ten years of tension: Single-molecule dna mechanics. Nature 2003;421:423–427. [PubMed: 12540915]
24. Cheng W, Lohman TM, Murphy MC, Rasnik I, Ha T. Probing single-stranded dna conformational flexibility using fluorescence spectroscopy. Biophysical Journal 2004;86:2530–2537. [PubMed: 15041689]
25. Jackson NM, McPherson LD, Potter AB, Spain EM, Allen MJ, Kelley SO, Barton JK, Hill MG. Orienting dna helices on gold using applied electric fields. Langmuir 1998;14:6781–6784.
26. Swan AK, Goldberg BB, Moiseev L, Unlu S, Cantor CR. Dna conformation on surfaces measured by fluorescence self-interference. PNAS 2006;103:2623–2628. [PubMed: 16477000]
27. Roodenko K, Vermeeren V, Williams OA, Daenen M, Douheret O, D'Haen J, Hardy A, Van Bael MK, Hinrichs K, Cobet C, VandeVen M, Ameloot M, Haenen K, Michiels L, Esser N, Wenmackers S, Pop SD, Wagner P. Structural and optical properties of dna layers covalently attached to diamond surfaces. Langmuir 2008;24:7269–7277. [PubMed: 18558777]
28. Cui Y, Smith SB, Bustamante C. Overstretching b-dna: The elastic response of individual double-stranded and single-stranded dna molecules. Science 1996;271:795–799. [PubMed: 8628994]
29. Siggia ED, Bustamante C, Marko JF, Smith SB. Entropic elasticity of λ-phage dna. Science 1994;265:1599–1600. [PubMed: 8079175]
30. Fujimoto BS, Schurr JM. The distribution of end-to-end distances of the weakly bending rod model. Biopolymers 2000;54:561–571. [PubMed: 10984407]
31. Sturm J, Tinland B, Pluen A, Weill G. Persistence length of single-stranded dna. Macromolecules 1997;30:5763–5765.
32. Gouy GJ. Sur la constitution de la charge Électrique a la surface d'un Électrolyte. J de Phys 1910;9:457–468.
33. Chapman DL. A contribution to the theory of electrocapilarity. Philos Mag 1913;25:475–481.
34. Crc handbook of chemistry and physics. 44.
35. Ohshima H, Kondo T. Electrostatic double-layer interaction between two charged ion-penetrable spheres: An exact solvable model. J Colloid Interface Sci 1993;155:499–505.
36. Ohshima H, Kondo T. Electrostatic interaction of aan ion-penetrable sphere with a hard plate: Contribution of an image interaction. J Colloid Interface Sci 1993;157:504–508.
37. Feig M, Pettitt BM. Structural equilibrium of dna represented with different force fields. Biophysical Journal 1998;75:134–149. [PubMed: 9649374]
38. Feig M, Pettitt BM. Experiment vs force fields: Dna conformation from molecular dynamics simulations. J Phys Chem B 1997;101:7361–7363.
39. Kulkarni A, McFaddin D, Merrick-Mack J, Ramachandran R, Beaucage G, Galiatsatos V. Persistence length of short-chain branched polyethylene. Macromolecules 2008;41:9802–9806.

40. Baumgartnet A, Binder K. Monte carlo studies on the fleely jointed polymer chain with excluded volume interaction. J Chem Phys 1979;71:2541–2545.

41. Flory, Paul J. Statistical Mechanics of Chain Molecules. Interscience; New York: 1969.

42. de Gennes, Pierre-Gilles. Scaling Concepts in Polymer Physics. Cornell Unversity Press; Ithaca: 1979.

43. Pang DW, Zhang ZL, Zhang RY. Orientation on gold by ec-stm. Bioconjugate Chem 2002;13:104–109.

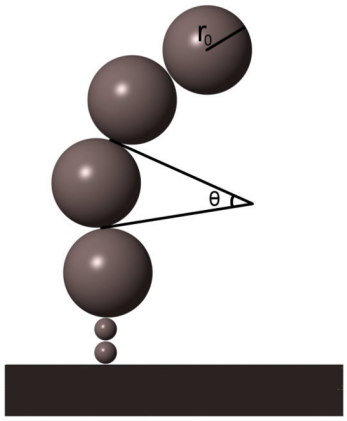

Figure 1.
Discretized worm like chain model near a surface.

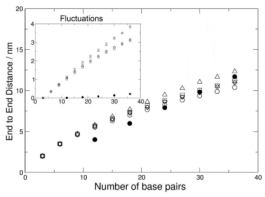

Figure 2.

Average end to end distance vs number of base pairs. The salt concentration is fixed at 0.14 M. The circle is ssDNA, square is ssDNA near a dielectric surface, diamond is ssDNA near a conducting surface, triangle is ssDNA near a dielectric surface with a $-0.36\ e^{-}$ per nm^2 (positive) charge, upsidedown triangle is ssDNA near a conducting surface with a 50 mV voltage and the filled circle is dsDNA. The errors are smaller than the symbols used.

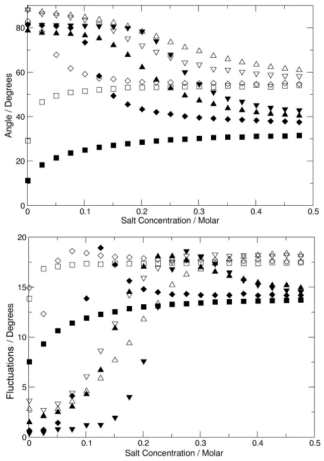

Figure 3.

Average angle vs salt concentration. All molecules are 18 base pairs long. Symbols for dsDNA are filled, and ssDNA are empty. Square is a neutral dielectric surface, diamond is a zero voltage conducting surface, triangle is a dielectric surface with a $-0.36\ e^{-}$ per nm^2 (positive) charge, and upsidedown triangle is a conducting surface with a 50 mV voltage

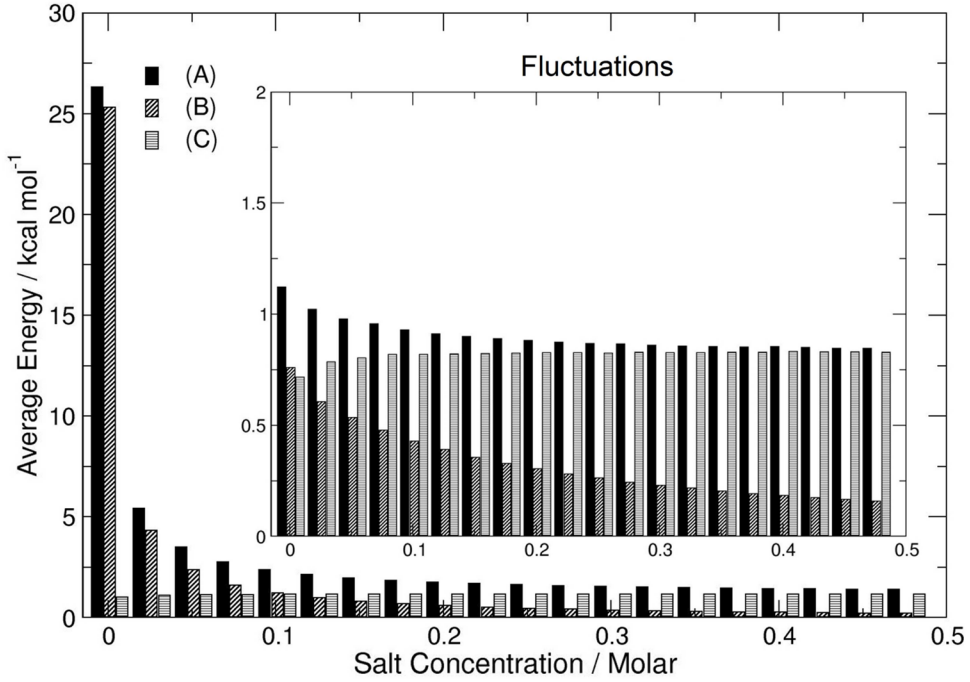

Figure 4.

Different energy contributions for different salt concentrations. The molecules are dsDNA and the surface is a dielectric. (A) Total Energy. (B) Energy due the image. (C) Energy due the internal bending.

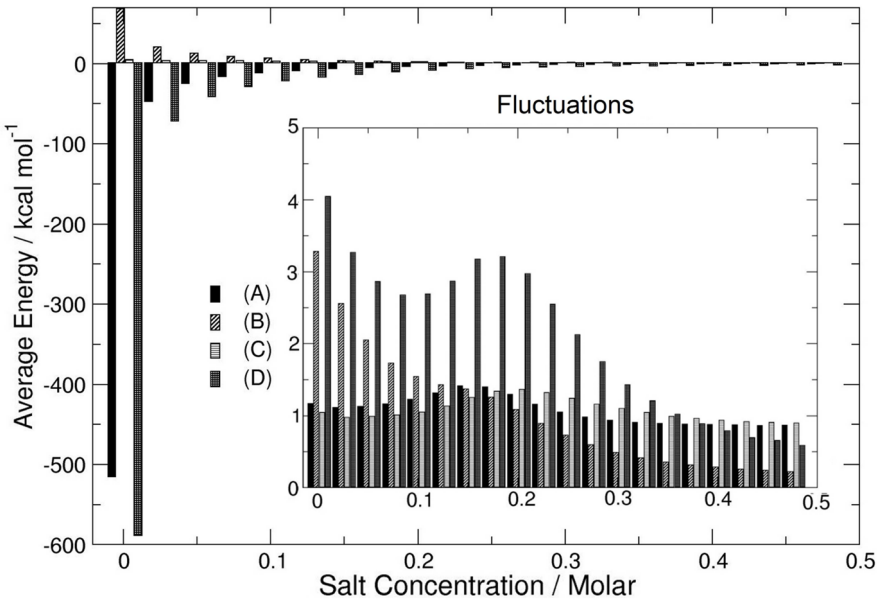

Figure 5.

Different energy contributions for different salt concentrations. The molecules are dsDNA and the surface is a dielectric with a charge of $-0.36\ e^{-}$ per nm^2. (A) Total Energy. (B) Energy due the image. (C) Energy due the internal bending. (D) Energy due the charge of the plate.

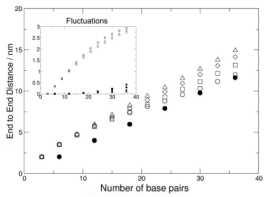

Figure 6.

Average end to end distance vs number of base pairs. The salt concentration is fixed at 0.14 *M*. The surface is a dielectric. Symbols for dsDNA are filled, and ssDNA are empty. Circle is at 0.01 molecules per nm^2, square is at 0.10 molecules per nm^2, diamond is at 0.15 molecules per nm^2 and triangle is at 0.20 molecules per nm^2.

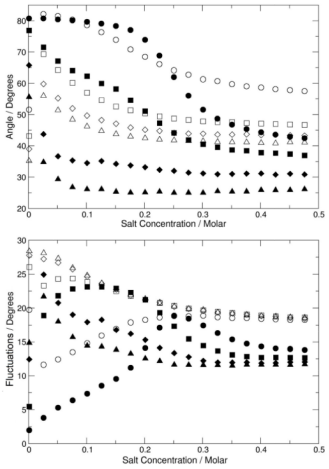

Figure 7.
Average angle vs salt concentration. All molecules are 18 base pairs long. The surface is a conductor with a 50 *mV* voltage. Symbols are the same as the preceding figure.

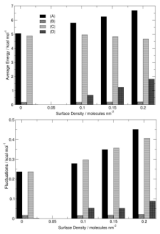

Figure 8.
ssDNA energy contributions for different molecular surface densities. The surface is a dielectric, the number of base pairs is fixed at 18 and the salt concentration is 0.14 *M*. (A) Total Energy. (B) Energy due the image. (C) Energy due the internal bending. (D) Energy due the neighbors.

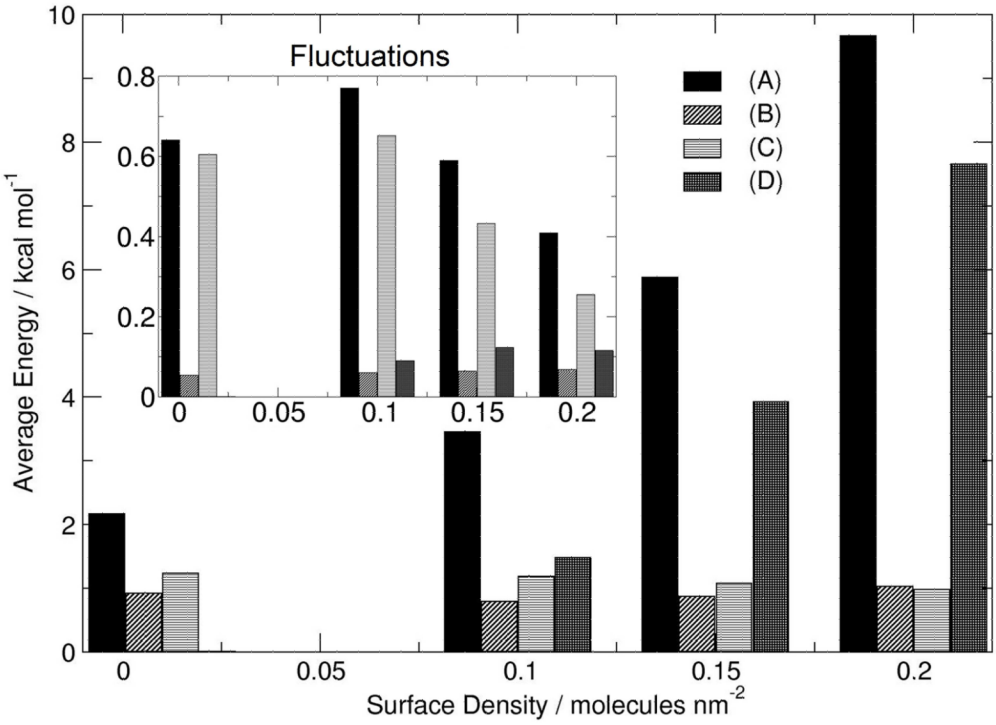

Figure 9.

dsDNA energy contributions for different molecular surface densities. The surface is a dielectric, the number of base pairs is fixed at 18 and the salt concentration is 0.14 *M*. (A) Total Energy. (B) Energy due the image. (C) Energy due the internal bending. (D) Energy due the neighbors.

Table 1

The effective exponents for the simulation data in Fig 2

Surface Type and charge (potential)	2ν
No Surface	1.200 ± 0.015
Conductor, No Potential	1.258 ± 0.014
Dielectric, No Charge	1.271 ± 0.018
Conductor, $+50mV$	1.294 ± 0.026
Dielectric, $-0.36e^{-}/nm^{2}$	1.421 ± 0.017